Geotechnical and Geophysical Site Characterisation 5 – Lehane, Acosta-Martínez & Kelly (Eds)

Evaluation of DMT-based liquefaction triggering curves based on field case histories

K.M. Rollins & T.K. Remund
Brigham Young University, Provo, Utah, U.S.A.

S. Amoroso
IstitutoNazionale di Geofisica e Vulcanologia, L'Aquila, Italy

ABSTRACT: Liquefaction is commonly evaluated using in-situ tests such as the cone penetration test (CPT) and the standard penetration test (SPT). However, these tests are relatively insensitive to a number of factors that are known to influence liquefaction resistance such as aging, stress history, overconsolidation, and horizontal earth pressure. In contrast, the flat blade dilatometer test is much more sensitive to these parameters and could potentially provide liquefaction resistance evaluations which can account for these factors. Three methods are available for predicting liquefaction resistance based on the DMT horizontal stress index K_D; however, their accuracy is poorly defined. To provide more direct evidence regarding the validity of the various approaches, DMT data has been collected at sites where liquefaction has and has not occurred in various earthquakes. The data set includes sites in California, Taiwan, New Zealand and Italy. In several cases, the sites were subjected to multiple earthquakes which did and didn't induce liquefaction. The *CRR* vs K_D curve is relatively well constrained for K_D values less than about 4. Both the Tsai et al. (2009) and Robertson (2012) curves provide reasonable triggering boundaries within this range. In contrast, the Monaco et al. (2005) curve is somewhat unconservative with liquefaction points below the curve. For K_D values greater than 4.0 there is insufficient data to determine which of the three triggering curves is most appropriate. Additional testing is necessary at sites with K_D greater than 4.0 where *CSR* is higher than 0.20 to define the triggering curve in this region.

1 INTRODUCTION

1.1 *Background*

Liquefaction is commonly evaluated using in-situ tests such as the standard penetration test (SPT) and the cone penetration test (CPT). These evaluation procedures have been developed by determining the penetration resistance at field sites which did or did not exhibit surface manifestation of liquefaction during earthquakes. The cyclic stress ratios (*CSR*), τ/σ'_o, for each of these sites were then plotted versus penetration resistance and a boundary or "triggering" curve was drawn to separate the points which liquefied from those that did not. The boundary curve then defines the cyclic resistance ratio (*CRR*), τ/σ'_o, required to induce liquefaction for that earthquake magnitude. Liquefaction triggering curves based on SPT have been developed by Youd et al. (2001), Cetin et al. (2004), and Boulanger & Idriss (2016). Curves based on the CPT have been developed by Robertson & Wride (1998), Idriss & Boulanger (2006), and Boulanger & Idriss (2016).

Unfortunately, both the SPT and CPT are relatively insensitive to a number of factors that are known to influence liquefaction resistance such as aging, stress history, overconsolidation, and horizontal earth pressure coefficient, K_o (Jamiolkowski & Lo Presti 1998, Lee et al. 2011, Marchetti 2015). In contrast, the flat blade dilatometer (DMT) test is much more sensitive to these parameters and could potentially provide liquefaction resistance evaluations that better account for these factors.

As noted by a number of researchers (e.g. Ishihara et al. 1977, Seed 1979), the liquefaction resistance of sand clearly increases as the K_o value increases. Although some researchers contend that K_o effects are reasonably considered in *CRR* vs q_{c1} evaluations (Salgado et al. 1997), other investigators have found that both the *CRR* vs q_{c1} and *CRR* vs $(N_1)_{60}$ curves were conservative without consideration of K_o effects (Harada et al. 2008). Harada et al. (2008) recommend a suite of *CRR* vs q_{c1} curves to properly account for K_o effects.

This issue is particularly important in evaluating liquefaction resistance after ground improvement because ground improvement typically increases both the soil density and K_o. If beneficial effects from increases in K_o can be relied upon, then the cost of liquefaction remediation could be reduced. Liquefaction triggering correlations based on the

horizontal stress index, K_D,from the DMT (Marchetti 1980) have the potential to address this problem.

Several investigators have developed methods for predicting liquefaction resistance (*CRR*) based on the DMT K_D. In contrast to liquefaction triggering curves based on $(N_1)_{60}$, q_{c1}, or$V_{S,}$, most triggering curves based on K_D were not developed directly from field performance data owing to the paucity of data. Instead researchers developed triggering curves using indirect correlations with relative density or correlations between K_D and q_{c1}or $(N_1)_{60.}$ To provide more direct evidence regarding the validity of the various approaches, DMT data has been collected at sites where liquefaction has and has not occurred in various earthquakes.

2 AVAILABLE LIQUEFACTION TRIGGERING CURVES

Correlations for predicting liquefaction resistance (*CRR*) based on the DMT K_D value have been proposed by three investigators: Monaco et al. (2005), Tsai et al. (2009), and Robertson (2012). This section summarizes the procedures used by each of these researchers and the resulting correlation equation.

2.1 *Monaco et al. (2005) Triggering Curve*

Because of the lack of$K_D$measurements at liquefaction sites, Monaco et al. (2005) used relative density as an intermediate variable to develop *CRR* vs K_D curves. For example, SPT-based liquefaction triggering curves developed by Youd et al. (2001) were used to develop a *CRR* vs. D_r curve using correlations between *SPT N* and D_r proposed by Gibbs & Holtz (1957) for a variety of vertical effective stresses. Thereafter, a correlation between K_D and D_r was used to develop the *CRR* vs K_D curve. A similar approach was used with the CPT-based liquefaction triggering curve proposed by Youd et al. (2001) and the resulting *CRR* vs K_D curve was quite similar to the curve based on the SPT-based correlation.

Finally, the following best-fit polynomial equation was developed to definean average *CRR* as a function of K_D:

$$CRR=0.0107K_D^3–0.0741K_D^2+0.2169K_D–0.1306 \quad (1)$$

This curve is plotted in Figure 1, and it is defined for clean sands and $K_D > 2$ considering also that Equation (1) computes negative *CRR* values for $K_D \approx 0.9$. Of course, the difficulty in using this approach is that the uncertainty associated with using two correlations with D_r would be expected to lead to greater uncertainty in the position of the *CRR* vs K_D curve.

2.2 *Tsai et al. (2009) Triggering Curve*

To avoid the problem of using an intermediate variable like D_r to develop a *CRR*-K_D correlation, Tsai et al. (2009) developed direct correlations between CPT q_{c1} and K_D as well as SPT $(N_1)_{60}$ and K_D. These correlations were developed based on companion soundings at a number of test sites in Taiwan. Based on results from both the SPT-based and CPT-based correlations in their investigations, the following equation average curve was developed defining *CRR* vs. K_D:

$$CRR = exp((K_D/8.8)^3-(K_D/6.5)^2+(K_D/2.5)-3.1) \quad (2)$$

which is also plotted in Figure 1. This curve is defined for clean sands and for $K_D > 1$. Although the two curves are in reasonable agreement for K_D values less than about 3, the curves diverge significantly at higher K_D values. The Monaco et al. (2005) curve yields significantly higher liquefaction resistance for a given K_D.

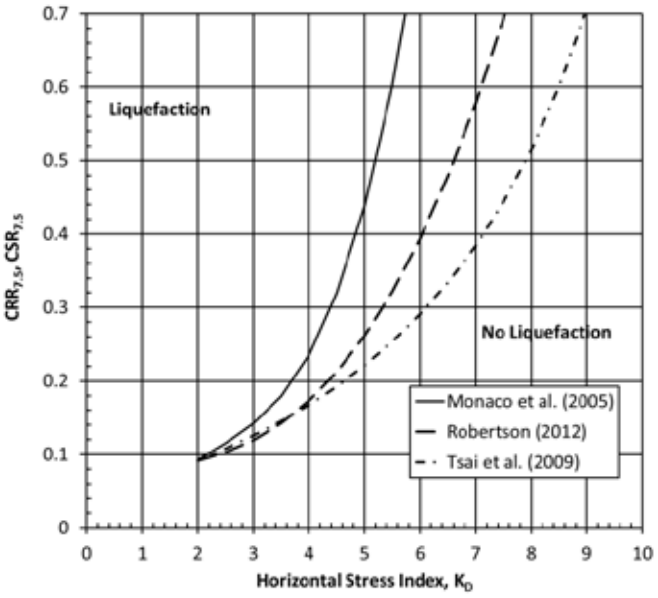

Figure 1. Comparison of DMT-based liquefaction triggering curves proposed by various researchers.

2.3 *Robertson (2012) Triggering Curve*

As part of his Mitchell lecture, Robertson (2012) proposed a third *CRR* vs K_D curve. This curve was based on a simpler correlation developed fromthe data set of companion CPT and DMT soundings developed by Tsai et al. (2009) indicating that K_D is approximately equal to $Q_{tn,cs}$/25 where $Q_{tn,cs}$ ($\approx q_{c1N,cs}$) is the clean sand equivalent cone resistance and is dimensionless. However, this correlation is highly approximate and there is significant scatter about the best-fit line.

The *CRR* vs K_D curve is defined based on the equation:

$$CRR = 93(0.025K_D)^3 + 0.08 \quad (3)$$

Equation (3) is defined for $I_D > 1.2$ and $2 < K_D < 6$. Once again, this curve is in reasonable agreement with the other two curves for K_D values less than about 3, but diverges from the other curves at higher values. Generally, the Robertson (2012) curve plots about mid-way between the Monaco et al. (2005) curve and the Tsai et al. (2009) curve.

3 COLLECTION AND PROCESSING OF AVAILABLE DATA

3.1 *Sources of Data*

Because of the significant discrepancies between the *CRR* vs. K_D curves proposed by various researchers, it will be necessary to appeal to field performance data to sort out the reliability of the various curves. Although relatively few DMT tests have been performed in post-earthquake investigations, some information is available and additional test data is being accumulated with additional earthquakes. As part of this study, a detailed literature review was undertaken to collect available DMT data. The largest data set was provided by Reyna (1991) (see also Reyna & Chameau, 1991) and included 32 tests at 5 sites in the Imperial Valley of California subjected to the the1979 M6.5 Imperial Valley earthquake, the 1981 M5.9 Westmorland earthquake, and the 1987 M6.5 Superstition Hills earthquake. These results were particularly valuable in identifying the liquefaction triggering boundary as some sites did not liquefy in the smaller event but did in the larger event. In addition, Reyna (1991) provided test data at 5 sites in the San Francisco Bay area subjected to the 1989 M6.9 Loma Prieta earthquake.

Additional DMT testing was performed by Hryciw et al. (1998) at 5 sites on Treasure Island and 5 sites in Santa Clara following the Loma Prieta Earthquake. Furthermore, Mitchell et al. (1994) report DMT test results at foursites in the SF Bay area while Rollins et al. (2015) and Faris & DeAlba (2000) each report tests for one site on Treasure Island subjected to the Loma Prieta Earthquake. An additional DMT data point was provided by Kung et al. (2011) for a site subjected to the M6.1 earthquake in Taiwan. Lastly, two data points were provided by investigations conducted by Amoroso et al. (2015) following the earthquake sequence near Christchurch, New Zealand and one from investigations at Mirabello, Italy after the M5.9 2012 Emilia-Romagna earthquake.

In many cases, CPT and V_s data has also been collected at sites where DMT testing has been performed in post-earthquake investigations. These data could be potentially useful in evaluating hybrid triggering curves which involve two in-situ measurements, such as the procedure proposed by Marchetti (2015) which uses both q_c from a CPT and K_D from the DMT. Fines contents and index tests were available in some cases along with the soil classification symbol according to the Unified Soil Classification System. Nevertheless fines content corrections are not included in DMT liquefaction triggering curves. The implementation of the *CRR*-K_D case history database could support the introduction of a more consistent liquefaction curve that could also consider the fine content influence using the material index I_D. We have included silty sand and sandy silt data points regardless of fines content to this point.

The DMT data set is clearly dominated by results from the Loma Prieta earthquake and by sites in California. Additional test data for other earthquakes and other geological settings would be very desirable. In so far as we can determine, all the sites described previously involve Holocene deposits. Some additional DMT data is available for older sediments in the New Madrid Seismic Zone and the Charleston, South Carolina area. However, these sites have been excluded at the present time as we consider how to adjust the results for aging effects. After adjustment for aging, these sites could potentially be included as data points for the same triggering curve as we routinely account for different magnitudes which are normalized to $M_w = 7.5$ using magnitude scaling factors.

3.2 *Evaluation of average values and CSR*

For each site where liquefaction occurred an average K_D value was taken from the liquefied layer. Where several depth ranges were given, the K_D value corresponding to each range was plotted throughout the liquefied layer. For sites where liquefaction did not occur average K_D values for several layers were plotted to capture the range of values involved.Fines content corrections were not taken into account in many cases owing to the lack of data in the evaluated studies.

CSR values for Figures 2, 3, and 4 were computed using the Youd et al. (2001), Idriss & Boulanger (2006), and Boulanger & Idriss(2016) methods. All methods used the *CSR* equation proposed by Seed and Idriss (1971).

$$CSR = 0.65\left(\frac{a_{max}}{g}\right)\left(\frac{\sigma_{vo}}{\sigma'_{vo}}\right)r_d/MSF \quad (4)$$

where a_{max} is the peak ground acceleration, σ_{vo} and σ'_{vo} are the total and effective vertical stresses, respectively, r_d is a stress reduction factor, and *MSF* is a magnitude scaling factor.The K_σ factor was not employed in computing *CSR* as this has not typically been done in developing the *CRR*-K_D correlations.

3.2.1 *Youd et al. (2001)Method:*

The Youdet al. (2001) method used Liao & Whitman's (1986) recommendations for stress reduction coefficients, r_d, as given by the following equations:

$$r_d = 1.0 - 0.00765z \quad \text{for z} \leq 9.15 \text{ m} \tag{5}$$

$$r_d = 1.174 - 0.0267z \quad \text{for } 9.15 \text{ m} < \text{z} \leq 23 \text{ m} \tag{6}$$

Magnitude scaling factors, *MSF*, were computed using the equation:

$$MSF = 10^{2.24}/M_w^{2.56} \tag{7}$$

3.2.2 *Idriss & Boulanger (2006) Method:*

Equations originally developed by Idriss (1999) were used to calculate the Boulanger & Idriss(2006) stress reduction coefficients and magnitude scaling factors. The stress reduction coefficients were computed using the equation:

$$r_d = \exp[\alpha(z) + \beta(z) \cdot M] \tag{8}$$

where:

$$\alpha(z) = -1.012 - 1.126\sin\left(\frac{z}{11.73} + 5.133\right) \tag{9}$$

$$\beta(z) = 0.106 + 0.118\sin\left(\frac{z}{11.28} + 5.142\right) \tag{10}$$

The magnitude scaling factors, *MSF*, were computed using the equation:

$$MSF = 6.9 \cdot \exp\left(\frac{-M}{4}\right) - 0.058 \leq 1.8 \tag{11}$$

3.2.3 *Boulanger & Idriss 2016 Method:*

The Idriss (1999) stress reduction coefficient equations were also used in the Boulanger and Idriss (2016) method. An overburden correction factor was first solved for to obtain MSF_{max}. $MSF_{max}$was then used to compute the overall *MSF* using the equations:

$$MSF = 1 + (MSF_{max} - 1)\left(8.64exp\left(\frac{-M}{4}\right) - 1.325\right) \tag{12}$$

where:

$$MSF_{max} = 1.09 + \left(\frac{q_{c1Ncs}}{180}\right)^3 \leq 2.2 \tag{13}$$

$$MSF_{max} = 1.09 + \left(\frac{(N_1)_{60cs}}{31.5}\right)^2 \leq 2.2 \tag{14}$$

The overburden correction factor, C_n, used in computing q_{c1} and $(N_1)_{60}$was computed using the equation:

$$C_N = \left(\frac{P_a}{\sigma'_v}\right)^m \leq 1.7 \tag{15}$$

where:

$$m = 1.338 - 0.249(q_{c1Ncs})^{0.264} \tag{16}$$

$$m = 0.784 - 0.0768\sqrt{(N_1)_{60cs}} \tag{17}$$

and

$$q_{c1N} = C_N \frac{q_c}{P_a} \tag{18}$$

4 COMPARISON OF TRIGGERING CURVES WITH FIELD PERFORMANCE DATA

As discussed in section 3, *CSR* values for each field data point were determined using the Youd et al. (2001) approach, the Idriss & Boulanger (2006) approach and the Boulanger & Idriss (2016) approach. *CSR*-K_D data pairs for these three approaches are plotted in Figures 2, 3, and 4, respectively. In these three figures, plots of the three proposed DMT-based liquefaction triggering curves are also shown along with the field performance data points.The solid red dots indicate liquefaction, while the open dots indicates no liquefaction.Generally, the Youd et al. (2001) approach gives the lowest *CSR* values, while the Idriss & Boulanger (2016) approach typically gave the highest.

For K_D values less than 4.0, where most of the data points are located, the liquefaction triggering boundary is fairly well constrained. Triggering curves proposed by Robertson (2012) and Tsai et al. (2009) seem to provide a reasonable boundary between liquefaction and no liquefaction points for most CSR assessment approaches. In contrast, the Monaco et al. (2005) curve seems to be somewhat unconservative with liquefaction points below the curve.

A review of the plots in Figures 2 through 4 indicates that there are very few data points indicating liquefaction where K_D is greater than 4. This does not necessarily mean that liquefaction will not occur at higher values, it simply means that data points have not yet been collected with high enough *CSR* values to produce liquefaction. Most of the data points with a K_D greater than 4 do not have *CSR* values above 0.175 and would not be expected to exhibit surface evidence of liquefaction based on any of the triggering curves. This observation points out the need to perform DMT tests at liquefaction sites where K_D is greater than 4 and where *CSR* is greater

than 0.2 to better define the boundary of the triggering curve.

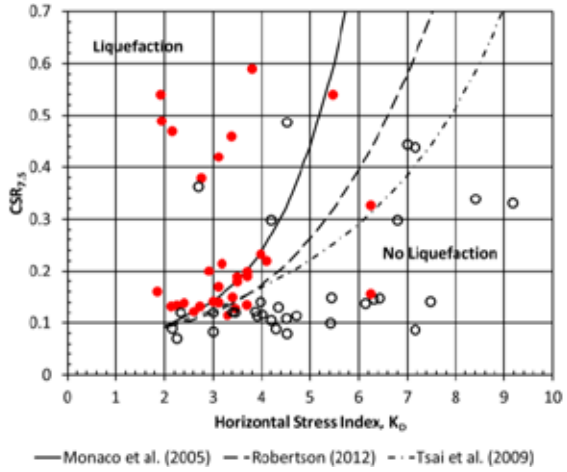

Figure 2. Comparison of proposed DMT-based liquefaction triggering curves with field performance data points using the Youd et al. (2001) approach for CSR.

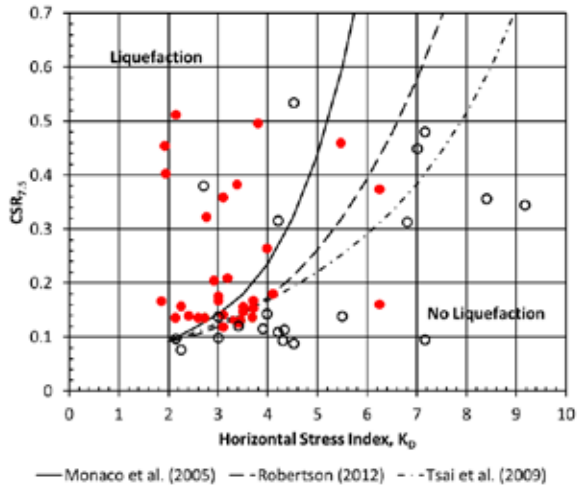

Figure 3. Comparison of proposed DMT-based liquefaction triggering curves with field performance data points using the Idriss and Boulanger (2006) approach for CSR.

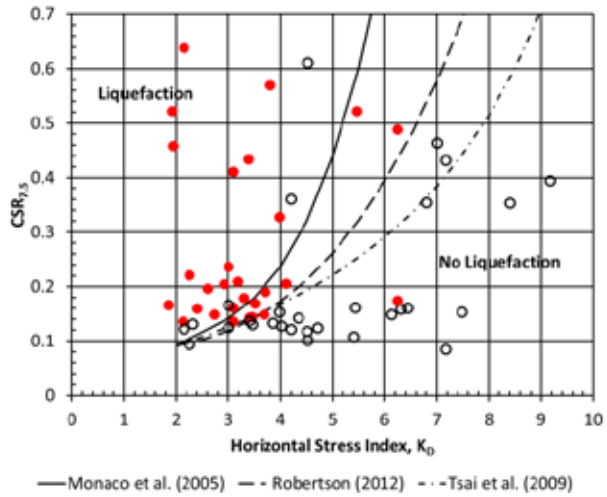

Figure 4. Comparison of proposed DMT-based liquefaction triggering curves with field performance data points using the Boulanger and Idriss (2016) approach for CSR.

There are also a few points with high *CSRs* that would be expected to liquefy based on all three DMT-based triggering curves but do not show signs of liquefaction. In some of these cases, the non-liquefiable surface layer may have been thick enough relative to the thickness of the liquefiable layer to prevent the manifestation of liquefaction effects at the surface as suggested by Ishihara (1985) and noted by Hryciw et al. (1998).

5 CONCLUSIONS

Despite the availability of liquefaction triggering curves based on CPT and SPT data, a DMT-based liquefaction triggering curve is highly desirable because it is more sensitive to aging, stress history, and horizontal earth pressure. These factors are particularly important when evaluating increased liquefaction resistance produced by ground improvement techniques when both the density and lateral pressure are increased.

The DMT-based field performance data provides reasonable discrimination between liquefaction and no liquefaction for K_D values less than 4.0. Both the Tsai et al. (2009) and Robertson (2012) curves provide reasonable triggering boundaries within this range. In contrast the Monaco et al. (2005) curve is somewhat unconservative with liquefaction points below the curve.

For K_D values greater than 4.0 there is currently insufficient data to determine which of the three triggering curves provide the most appropriate boundary. Additional testing is necessary at sites with K_D greater than 4.0 where CSR is higher than 0.20 to help define the triggering curve in this region.

6 ACKNOWLEDGEMENTS

Funding for this study was provided by US National Science Foundation grant no. CMMI-1408892. This support is gratefully acknowledged. The conclusions, interpretations, and opinions presented in this paper are those of the authors and do not necessary reflect the views of the sponsor.

7 REFERENCES

Amoroso, S., Monaco, P., Rollins, K.M., Holtrigter, M. & Thorp, A. (2015). Liquefaction assessment by seismic dilatometer test (SDMT) after 2010-2011 Canterbury earthquakes (New Zealand). *6th International Conference on Earthquake Geotechnical Engineering - 6ICEGE, 1-4 November 2015, Christchurch, New Zealand*.

Boulanger, R.W. & Idriss, I.M. 2016. CPT-Based Liquefaction Triggering Procedure. *J. Geotech. Geoenviron. Eng.*, 142(2), 11

Cetin, K.O., Seed, R.B., Der Kiureghian, A., Tokimatsu, K., Harder, L.F., Kayen, R.E. & Moss, R.E. 2004. Standard Penetration Test-Based Probabilistic and Deterministic Assessment of Seismic Soil Liquefaction Potential. *J. Geotech. Geoenviron. Eng.*, 130(12), 1314-1340.

Farris, J.R. & DeAlba, P. 2000. National Geotechnical Experimentation Site at Treasure Island, California. *National Geotechnical Experimentation Sites, GSP No. 93*, p. 52-68.

Gibbs, K.J. & Holtz, W.G. 1957. Research on determining the density ofsands by spoon penetration testing. *Proc. IV ICSMFE*, 1, 35-39.

Harada, K., Ishihara, K. Orense, R.P., & Mukai, J. 2008. Relations between penetration resistance and cyclic strength to liquefaction as affected by Kc–conditions. *Proc, Geotechnical Earthquake Engineering and Soil Dynamics IV*, Sacramento CA, Paper 111, 12pp (in CD–ROM).

Hryciw, R.D., Shewbridge, S.E., Kropp, Al, & Homolka, M. (1998). Post-earthquake investigations at liquefaction sites in Santa Cruz and on Treasure Island. *U.S. Geological Survey Prof.* Paper 1551-B, B165-B180.

Idriss, I.M. 1999. An update to the Seed-Idriss simplified procedure for evaluating liquefaction potential. *Proc. TRB Workshop on New Approaches to Liquefaction*, Publ. No. FHWA-RD-99-165, Federal Highway Administration.

Idriss, I. M., and Boulanger, R. W. (2006). Semi-empirical procedures for evaluating liquefactionpotential during earthquakes, *J. Soil Dynamics and Earthquake Eng.,* 26, 115–130.

Ishihara, K., Iwamoto, S., Yasuda, S., & Takatsu, H. 1977. Liquefaction of aniosotropically consolidated sand. *Prods. Ninth Int. Conf. on Soil Mech. and Found. Engrg.*, Japanese Society of Soil Mech. and Found. Engrg., Tokyo, Japan, Vol. 2, 261-264.

Ishihara, K. 1985. Stability of Natural deposits During Earthquakes. *Procs. 11th Intl. Conf. on Soil Mech. and Found. Engrg.*,Bakema, Rotterdam, Netherlands, Vol. 1, 321-376.

Lee, M., Choi, S., Kim, M. & Lee, W. 2011. Effect of Stress History on CPT and DMT results in Sand. *J .Engrg. Geology, Elsevier*, 117, 259-265.

Jamiolkowski, M. and Lo Presti, D.C.F. (1998). "DMT research in sand. What can be learned from calibration chamber tests".*1st Int. Conf.onSiteCharacterizationISC'98*, Atlanta. Oral presentation.

Jamiolkowski, M., Baldi, G., Bellotti, R., Ghionna, V. & Pasqualini, E. 1985. Penetration resistance and liquefaction of sands. *Proc. XI ICSMFE*, San Francisco, 4, 1891-1896.

Liao, S.S.C. & Whitman, R.V. 1986. Catalogue of liquefaction and non-liquefaction occurrences during earthquakes. *Res. Rep.*, Dept. of Civ. Engrg., Massachusetts Institute of Technology, Cambridge.

Marchetti, S. 1980. In Situ Tests by Flat Dilatometer. *J. Geotech. Engrg. Div., ASCE*, 106, No.GT3, 299-321.

Marchetti, S. 2015. Incorporating the Stress History Parameter K_D of DMT into the Liquefaction Correlations in Clean Uncemented Sands. *J. Geotech. Geoenviron. Eng.*, ASCE, 142(2).

Mitchell, J.K., Lodge, A.L., Coutinho, R.Q., Kayen, R.E., Seed, R.B.,Nishio, S. & Stokoe, K.H. 1994. Insitu test results from four LomaPrieta earthquake liquefaction sites: SPT, CPT, DMT and shearwave velocity. *Report No. UCB/EERC-94/04*, Earthquake EngineeringResearch Center, Univ. of California, Berkeley.

Monaco, P., Marchetti, S., Totani, G. & Calabrese, M. 2005. Sand liquefiability assessment by Flat Dilatometer Test (DMT). *Proc. XVI ICSMGE*, Osaka, 4, 2693-2697.

Reyna, F. & Chameau, J.L. 1991. Dilatometer Based Liquefaction Potential of Sites in the Imperial Valley. *Proc. 2nd Int. Conf. on Recent Adv. in Geot. Earthquake Engrg. and Soil Dyn.*, St. Louis, 385-392.

Reyna, F.A.M. 1991. In situ tests for liquefaction potential evaluation: Applicationto California data including data from the 1989 Loma Prietaearthquake. *Ph.D. Dissertation*, Purdue Univ. 502 p.

Robertson, P.K. 2012. Mitchell Lecture. Interpretation of in-situ tests - some insight. *Proc.4th Int. Conf. on Site Characterization ISC-4*, Porto de Galinhas - Brazil, 1, 3-24.

Robertson, P.K. & Wride, C.E. 1998. Evaluating cyclic liquefaction potential using the cone penetration test. *Canadian Geotech. J.,* 35(3), 442-459.

Rollins, K.M., Amoroso, S. & Hryciw, R. (2015). Comparison of DMT, CPT, SPT, and V_S based liquefaction assessment on Treasure Island during the Loma Prieta earthquake. *Procs. 3rd Intl. Conf. on the Flat Dilatometer, Rome, Italy*, 349-356.

Salgado, R., Boulanger, R. & Mitchell, J. 1997. Lateral Stress Effects on CPT Liquefaction Resistance Correlations. *J. Geotech. Geoenviron. Eng.*, 123(8), 726–735.

Seed, H.B., & Idriss, I.M. 1971. Simplified procedure for evaluating soil liquefaction potential. *J. Geotech. Engrg. Div.*, ASCE, 97(9),1249–1273.

Seed, H.B. 1979. Soil Liquefaction and Cyclic Mobility Evaluation for Level Ground during Earthquakes. *J. Geotech. Eng. Div., ASCE*, Vol. 105(2), 201-255.

Tsai, P., Lee, D., Kung, G. T. & Juang, C.H. 2009. Simplified DMT-based methods for evaluating Liquefaction Resistance of Soils. *J .Engrg.Geology, Elsevier*, 103, 13-22.

Kung, G. T., Lee, D. & Tsai, P. 2011. Examination of DMT-based methods for evaluating the liquefaction potential of soils. *Applied Physics & Engineering*, 12(11), 807-817.

Youd, T.L., Idriss, I.M., Andrus, R.D., Arango, I., Castro, G., Christian, J.T., Dory, R., Finn, W.D.L., Harder, L.F., Hynes, M.E., Ishihara, K., Koester, J.P., Liao, S.S.C., Marcuson, W.F., Martin, G.R., Mitchell, J.K., Moriwaki, Y., Power, M.S., Robertson, P.K., Seed, R.B., & Stokoe, K.H. 2001. Liquefaction Resistance of Soils: Summary Report from the 1996NCEER and 1998 NCEER/NSF Workshops on Evaluation of Liquefaction Resistance of Soils. *J. Geotech. Geoenviron. Eng.,* ASCE, 127(10), 817-833.